# Study on high-purity Titanium powder for biomedical application

C. G. DUMITRAS[a], R. CERNAT[b,*], T. STAMATE[b], M. VARDAVOULIAS[c]
[a]*Technical University "Gheorghe Asachi" of Iasi, Romania*
[b]*"Gr.T.Popa" University of Medicine and Pharmacy Iasi, Romania*
[c]*PyroGenesis SA, Lavrio, Greece*

Titanium is most commonly associated with jet engines and airframes, but the most recent researches indicate its applicability for fittings for prosthetic devices and artificial heart. Titanium castings are often more economical than small fabricated parts, metal injection moulded, stamped and forged parts. The paper presents an experimental factorial plan applied to a new process of obtaining high purity titanium powder in order to optimize this process and to control the amount of titanium powder in a range of specific diameters. The process is based on plasma atomization. The resulting titanium powder was used in obtaining titanium moulded posts. A FE analysis was carried out in order to compare the response of different types of materials to the behavior of titanium posts.

(Received July 19, 2014; accepted November 13, 2014)

*Keywords*: Titanium powder, Biomedical application, Optimize, Experimental data, Atomization

## 1. Introduction

Titanium castings are often more economical than small fabricated parts, metal injection moulded, stamped and forged parts. Other applications are: raw material for HIP process (turbine blades), medical (ends-prosthetics and implants for the replacement of bone defects), high quality filters for the purification of drinking waters, industrial effluents, waste from electro-chemical production, and diesel fuel and particulate emissions from industrial enterprises.

Titanium and its alloys have proven to be technically superior and cost-effective materials of construction for a wide variety of aerospace, industrial, marine and commercial applications. In North America, approximately 70% of the titanium consumed is utilized for aerospace applications. Due to the expansion of existing applications and the development of new uses, the greatest growth will occur in the industrial, marine and medicine sectors.

Once judged to be expensive, titanium is now more often seen to be an economical solution, considering its entire life cycle costs. The key to its cost-effective use is to utilize its unique properties and characteristics in the design rather than to substitute titanium for another metal. Titanium availability is not an issue, as it is the world's fourth most abundant structural metal.

## 2. Technologies for production of high-purity TITANIUM powder

Powder metallurgical solutions have stood the test in industrial application a continuous advancement and innovative products have opened new market segments.

The powder metallurgical processing route is useful for producing a wide range of both developmental and commercial materials for industrial applications. Techniques such as gas atomization, water atomization, centrifugal atomization, plasma atomization, mechanical attrition and alloying, melt spinning, rotating electrode process (REP), and a variety of chemical processes are used to produce metal powders. The metal powders are characterized by their morphology, which can be described as irregular, blocky or spherical, and powder size. The powder metallurgical route is often more economical in terms of cost, precision, and productivity than other processes such as casting and forging.

Processes for producing fine metal powders are listed in Fig. 1 [1].

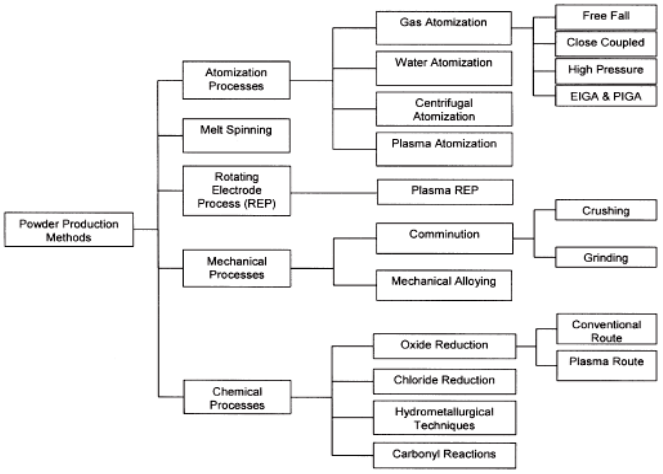


*Fig. 1. Different processes for powder production [1].*

The material powders manufacturing technologies depend on the mechanical behaviour of different materials. Titanium is becoming more widely used in an increasing array of applications. The delay in its widespread use and acceptance can be attributed to the inherent processing difficulties associated with its reactive nature. Although titanium parts can be manufactured with a variety of powder metallurgy (PM) technique [4] [5], the quality and the mechanical properties of the final components are often insufficient for the intended use. The presence of impurities such as chlorine, sodium, hydrogen, magnesium, nitrogen and oxygen, as well as the lubricants added to the starting powders, will affect the fatigue, the strength and the ductility of the part [6]. The methods to manufacture titanium powder can be summarized as: solid state reduction, electrolysis, atomization, mechanical comminution and chemical processes.

*Atomization* is one of the modern techniques who play an important role in many industrial processes from oil or waste combustion to ceramic powder synthesis is the atomization process. Most atomizers are one of three main types, pressure atomizers, two-fluid atomizers, and rotary cup atomizers. Pressure atomizers are relatively simple and inexpensive, but are easily plugged by solids and cannot handle high viscosity liquids. Two-fluid atomizers are slightly less prone to plugging, but still have difficulty handling viscous fluids and tend to be expensive to operate because of the need for high-pressure atomizing gas or steam. Rotary cup atomizers can be effective, but have the major disadvantage of being more mechanically complex [18].

Atomization is a process in which molten metal is broken up into small droplets and rapidly frozen before the drops come into contact with each other or with a solid surface. This technique uses air, steam, or an inert gas to produce powders from molten metal. The particle shape is determined largely by the rate of solidification and varies from spherical, if a low heat capacity gas is employed, to highly irregular if water is used [11]. Atomization is the process used commercially to produce the largest tonnage of metal powders.

Among the metal powder manufacturing processes, atomization has become the dominant mode of powder fabrication. It is attractive because of its applicability to several alloys and because of the ease of process control [8].

Using Ti and other reactive metals in metal injection moulding and thermal spraying has been limited by difficulties in producing fine, flowable metal powders. ***Plasma Atomization*** is a new technology developed jointly by PyroGenesis Inc. of Montreal, Canada and LTEE (Hydra-Quebec) of Shawinigan, Canada that looks set to resolve these problems [15].

The momentum that a plasma torch can deliver has been overlooked for years. Non-transferred arc plasmas are widely used for the deposition of coatings, melting, gas heating, materials syntheses, and waste destruction. Plasmas are generated by introducing an electric discharge into an inert gas such as argon. Some of the argon is ionized and heated to temperatures as high as 11 000 $^0$K The remaining gas is heated by the ionized argon and can reach 2000-10 000 $^0$K. The basic concept behind the patented Plasma Atomization technology is to convert the electrical energy, supplied to a plasma torch, into kinetic energy. The high thermal energy generated by the plasma torch is converted into a high velocity jet of extremely hot inert gas. The high velocity ensures adequate atomization, while the extended high temperature zone allows the spheroidization process to be completed.

Furthermore, PyroGenesis Inc has developed a patented DC non-transferred plasma torch which maximizes the enthalpy content of the gas, while minimizing the erosion of the electrodes. The Plasma Atomization process consists of three DC plasma torches vertically inclined, into a common apex, where the metal feed is introduced and atomized in a single step operation (Fig. 2). For reactive metals such as titanium, it is preferable to use a wire as a starting material. Hence, metal wires can be melted and atomized in a single step, while avoiding the technical difficulties associated with the handling of a molten bath of titanium [7].

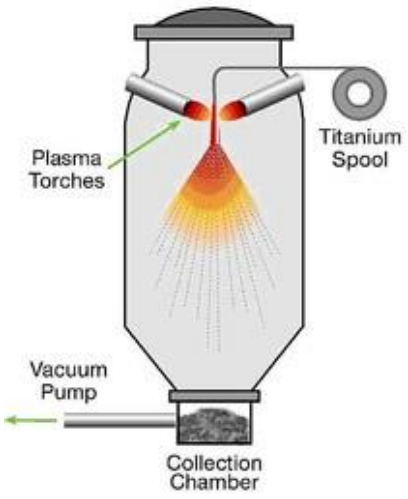


*Fig. 2. Plasma atomization.*

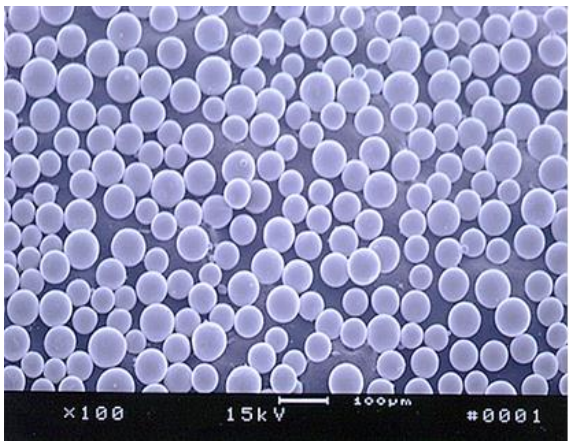


*Fig.3. Titanium powder.*

With the possibility of atomizing both molten metal streams and wires, the process is extremely versatile. All of the powders produced had an average diameter, $D_{50}$, which lies between 40 μm and 90 μm (Fig. 3). An average diameter of this order implies that an important fraction of the powder produced can be used for injection moulding applications (size range from 25 μm to 45 μm). In addition, the slightly coarser powder can be used for thermal spraying (e.g. typical Ti powders size range for Vacuum Plasma Spraying of 45÷75 μm). The problem that arise is to control the process parameters such as wire feed rate, current strength, gas flow rate and others in order to obtain a specific amount of titanium powder with size range located between controlled values.

The influence of the process parameters upon the size of titanium sphere size is expressed by mathematical equation obtained by an experimental design which is presented in the followings.

## 3. Experimental design for modelling the process

A *complete $2^k$ Factorial Design* was used for modelling the process of manufacturing the titanium powders by plasma atomization.

The use of an ***experimental design*** to determine the influence of the optimization factors upon the objective function is based on:

– minimum number of experiments;

– high precision of the resulting mathematical model

– uniform and equal distribution of the experiments all over the experimental domain of variation thus the objective function being defined on the entire domain.

A ***second order design*** is recommended because the variation of the independent variables cannot be defined by a linear approximation. Also, as the orientation of response surface toward the co-ordinate system axis is unknown, a ***central, composite and rotatable design*** is best suitable. Considering the optimization factors chosen for this study, a *$2^4$ design* with 31 combinations ($2^4$ factorial + star design +7 points (experiments) in the centre) is used [3], [10]. The variation levels of these factors are presented in the Table 1.

*Table 1. Coded and natural independent variables.*

| Nr. crt. | Coded Variable / Natural Variable | - 2 | -1 | 0 | 1 | 2 | Δ p |
|---|---|---|---|---|---|---|---|
| 1 | **Current strength** $x_1$ = I (A) | 120 | 155 | 190 | 225 | 260 | 35 |
| 2 | **Feed rate** $x_2$ = f (mm/min) | 400 | 525 | 650 | 775 | 900 | 125 |
| 3 | **Gas flow rate** $x_3$ = Q (l/min) | 72 | 79 | 86 | 93 | 100 | 7 |
| 4 | **Voltage** $x_4$ = U (V) | 96 | 102 | 108 | 114 | 120 | 6 |

The ***objective functions*** are calculated based on these optimization factors:

$$P_{75-45} = C_{P45} e^{a_1 I} e^{a_2 f} e^{a_3 Q} e^{a_4 U} \quad (1)$$

$$P_{<45} = C_{P25} e^{a_1 I} e^{a_2 f} e^{a_3 Q} e^{a_4 U} \quad (2)$$

These functions are used to determine the percentage variation for each size range of Ti spheres. Considering the following notations $Y_1=\ln P_{75\text{-}45}$ ; $Y_2=\ln P_{<45}$ ;$x_1$= I ; $x_2$=f; $x_3$=Q; $x_4$=U; $a_0$= $\ln Cp_{75\text{-}45}$; $b_0=\ln C_{P<45}$ and taking logarithms of both sides of the equations (1, 2) the following relations are obtained:

$$Y_1 = a_0 + \sum_{i=1}^{i=5} a_i x_i \quad (3)$$

$$Y_2 = b_0 + \sum_{i=1}^{i=5} b_i x_i \quad (4)$$

In order to increase the precision of approximations of the objective functions it is recommended to change the functions (3) and (4) in Taylor series, reducing the unneeded terms. Thus one obtains:

$$\begin{aligned} Y_1^* &= a_0^* + \sum_{i=1}^{i=5} a_i^* x_i + \sum_{i=1;i<j}^{i=4;j=5} a_{ij} x_i x_j + \sum_{i=1}^{i=5} a_{ii} x_i^2 \\ Y_2^* &= b_0^* + \sum_{i=1}^{i=5} b_i^* x_i + \sum_{i=1;i<j}^{i=4;j=5} b_{ij} x_i x_j + \sum_{i=1}^{i=5} b_{ii} x_i^2 \end{aligned} \quad (5)$$

The coded variables from the Table 1 are obtained with the following equation:

$$x_{ic} = \frac{x - x_{nm}}{\Delta p} \quad (6)$$

where: $x_{ic}$=coded variable; $x_{nm}$=average natural variable; Δp=increment.

In order to estimate the coefficients from equations (1) the method of smallest squares was applied. In accordance to that, by the using of the generic relation (5) for the objective functions, the standard deviation ε between the objective function responses, $Y_r$* (recorded for all experiments) and the corresponding Y* values must be minimum, i.e.:

$$Y^* = b_0 + \sum_{i=1}^{i=5} b_i x_i + \sum_{\substack{i=1 \\ i<j}}^{\substack{i=4 \\ j=5}} b_{ij} x_i x_j + \sum_{i=1}^{i=5} b_{ii} x_i^2 \quad (7)$$

$$\varepsilon = \sum_{n=1}^{n=31} \left( Y_{r\,n}^* - Y_n^* \right)^2 = \min \quad (8)$$

To achieve the condition (8), the following equations system (9) must be fulfilled:

$$\frac{\partial \varepsilon}{\partial b_0} = 0;\ \frac{\partial \varepsilon}{\partial b_i} = 0;\ \frac{\partial \varepsilon}{\partial b_{ij}} = 0;\ \frac{\partial \varepsilon}{\partial b_{ii}} = 0 \quad (9)$$

After solving the equations (9), the following relations for coefficients estimations of approximate polynom result:

$$b_0 = 0.142857 \sum_{n=1}^{n=31} Y^*_n - 0.035714 \sum_{n=1}^{n=31} \left( \left( \sum_{i=1;n=1}^{i=4;n=31} x_{ic}^2 \right) Y^*_n \right)$$

$$b_i = 0,041667 \sum_{i=1;n=1}^{i=5;n=32} x_{ic} Y^*_n$$

$$b_{ij} = 0,0625 \sum_{\substack{i=1;n=1 \\ i<j}}^{i=5;n=32} x_{ic} x_{jc} Y^*_n$$

$$b_{ii} = 0,03125 \sum_{i=1;n=1}^{i=5;n=32} x_{ic}^2 Y^*_n + 0,003720 \sum_{n=1}^{n=32} \left( \left( \sum_{i=1;n=1}^{i=5;n=32} x_{ic}^2 \right) Y^*_n \right) - 0.035714 \sum_{n=1}^{n=32} Y^*_n \quad (10)$$

where: $Y_{r\,n}$* = the objective function response;
$x_{in}$, $x_{jn}$ = the coded value of independent variables, according to Table 1.

The resulting coefficients and respectively constants are presented in Table 2. The 2D graphs and the 3D response surfaces which indicate the interdependence between the optimization factors and the process are presented in Figs. 4, 5 and 6.

*Table 2. Final shape of the objective functions.*

| No. | Objective function and it's coefficients | Exponent | Exponents expressions |
|---|---|---|---|
| 1 | $P_{75\text{-}45}$ $C_{P75\text{-}45} = e^{3.43088}$ | $a_1$ | -0.0046369 - 6.3152*10$^{-6}$ f - 6.3676*10$^{-6}$ I -0.000077 Q + 0.00016 U |
| | | $a_2$ | 0.001860084+ 3.29233*10$^{-6}$ f - 6.3152*10$^{-6}$ I - 0.000015 Q - 0.000036 U |
| | | $a_3$ | 0.00104-0.0000149923 f-0.0000766094 I+0.000514378 Q-.000556525 U |
| | | $a_4$ | -0.0117459-0.000035 f+0.0001635 I-0.000557 Q+0.000257539 U |
| 2 | $P_{<45}$ $C_{P<45} = e^{-15.724}$ | $a_1$ | 0.00595599 - 5.437428*10$^{-6}$ f -0.0000375 I + 0.0001475 Q + 0.0000229 U |
| | | $a_2$ | 0.01509 -1.859*10$^{-6}$ f - 5.437428*10$^{-6}$ I - 0.0000375 Q - 0.0000803 U |
| | | $a_3$ | 0.219235 -0.0000375 f +0.0001475 I- 0.00043 Q-0.0014 U |
| | | $a_4$ | 0.0783707-0.00008 f + 0.000023 I-0.0014 Q +0.00038 U |

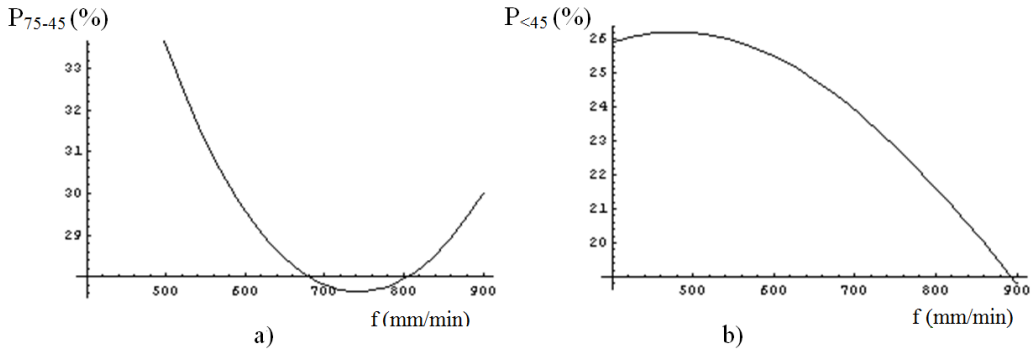


| Working conditions | | |
|---|---|---|
| I(A) | Q (l/min) | U (V) |
| 260 | 86 | 108 |

*Fig. 4. The variation of the particle size (%) with the feed rate: a) size range 75 to 45 μm b) less than 45 μm.*

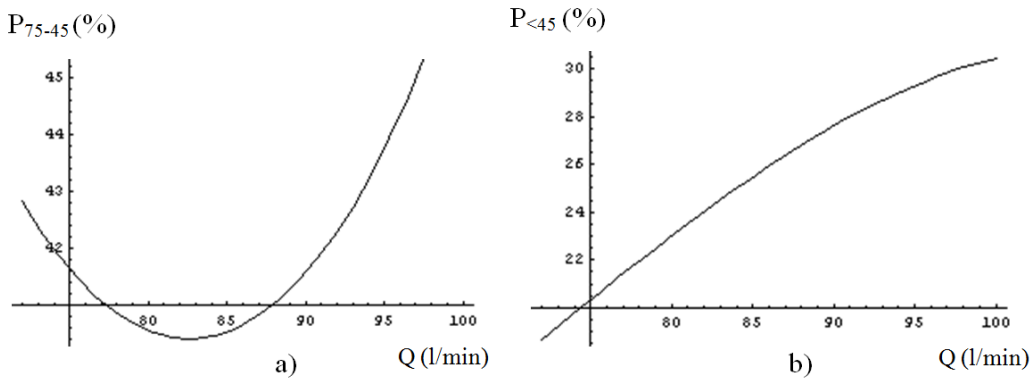


| Working conditions | | |
|---|---|---|
| I(A) | f (mm/min) | U (V) |
| 260 | 400 | 108 |

*Fig. 5. The variation of the particle size (%) with the gas flow rate: a) size range 75 to 45 μm b) less than 45 μm.*

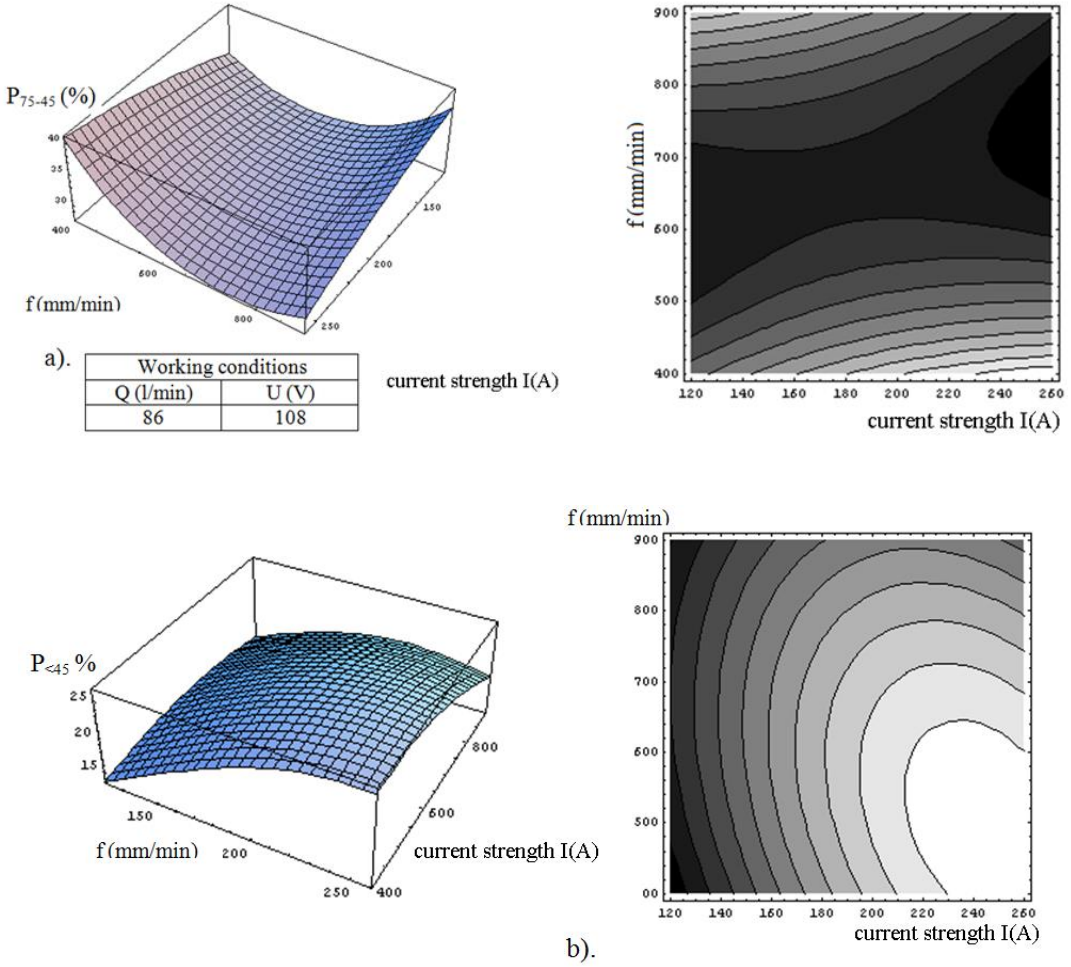


| Working conditions | |
|---|---|
| Q (l/min) | U (V) |
| 86 | 108 |

*Fig. 6. The variation of the particle size (%) with the current strength and feed rate a) size range 75 to 45 μm b) less than 45 μm.*

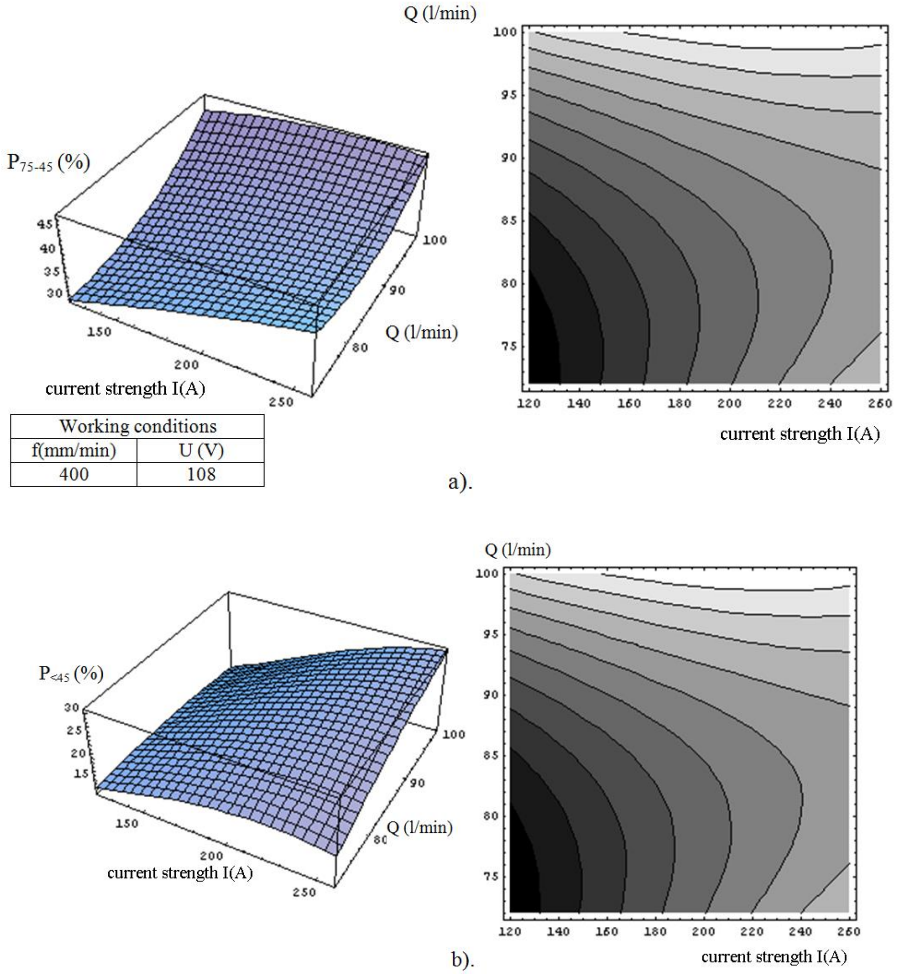


*Fig. 7. The variation of the particle size (%) with the current strength and gas flow rate a) size range 75 to 45μm b) less than 45 μm.*

## 4. Response analysis

The 2D graphs provide information about the influence of each process parameter on obtaining titanium powders with certain structure, referring to the percentage of the powders with the specified size range. The following conclusions can be drawn from the experimental data:

### 4.1 Response surfaces 2D

In the case of the Ti wire feed on producing the powder the following conclusion can be drawn: when the feed increases, it determines a decreasing of the amount of powder with diameters between 75 and 45 μm. This is justified by the fact that the wire displacement speed increases with the feed and consequently decreasing the time the wire is displaced through the working area. Subsequently the amount of heat changed between the medium and wire is reduced and therefore the wire temperature decreases, affecting the atomization process. A constancy of the phenomena can be observed until 550-600 mm/min, and then a dramatic decreasing occurs, more pronounced for the particles with size range 75-45 μm, followed by a slow variation, below 1% and corresponding to a feed value of 700 mm/min. It can be concluded that the feed increasing has a slight negative influence for the 75-45 μm particles and a little more pronounced influence for particles less than 45 μm.

The gas flow variation, i.e. the argon gas, has a positive influence. An increasing of the gas flow increases the amount of 75-45 μm powder particles. This increasing is even more pronounced for diameters under 45 μm. This is a strong influence and it can be explained by the fact that when the flow grows the flame changes its position, so that its consistency and dimensions are changing close to the working area. Thus, more heat in the working area is generated with a positive influence on the temperature fields and implicitly on the atomization.

### 4.2 Response surfaces 3D

The influences shown in the 2D graphs remain, with the specification that the influence of the intensity on the process is diminished with the increasing of the wire feed. Best results occur at low feed and great intensity. These influences are more pronounced for the 45 - 75 μm size range. For lower current intensity, the feed has virtually no influence on the process.

A similar level of influence is also noted for the interacting between the current intensity and gas flow, i.e. the variation of both parameters has a positive influence on the process, meaning that the amount of powder particles with diameters less than 75 μm increases. The 3D response surfaces also show that at lower levels of gas flow, when the intensity varies the influence is stronger for 45 - 75 μm particles and remains virtually constant for particles with diameters less than 45 μm. The area of maximum appears at maximum flow and maximum intensity.

Based on the aspects mentioned above we can conclude that the variable process parameters have a distinct and complex influence on the selected size ranges - 45-75 μm and less than 45 μm. The hierarchy of the independent variables resulting from the experiment is: current intensity, voltage, gas flow and wire feed. Current intensity, voltage and gas flow have a positive influence, while the wire feed has a negative influence on particle size.

### 4.3 High purity Titanium powder biomedical application

There are many types of biomedical applications for titanium powder. Usually, this powder is moulded in a complex shaped mould, pressed at high pressure and then heated at over 1300°C thus obtaining the required strength. Recent developments use 3D printers in order to obtain complex shape with high purity titanium alloy. Some examples of biomedical applications for titanium powder are presented below.

*Fig. 8. Titanium mandible [9].*

The titanium alloy mandible was obtained using a 3 D printer (Fig. 8) [9]. The titanium implant is very complex, it has flexible joints, housings muscle nerves and veins, like a jaw bone. The implant is made up of thousands of layers of titanium powder heated and shaped by means of a laser [14].

*Fig. 9. Spinal implant [19].*

*Fig. 10. Implants for proximal humerus fracture humeral shaft [2].*

Two types of implants for elder people are presented in Figs. 9 and 10. In the first case, the system has a revolutionary modular connector fixed cross which gives the surgeon a variety of options positioning it without sacrificing more bone [19]. Fracture of the proximal humerus is the second most common upper extremity fracture and the third most common fracture in patients over 65 years after hip and distal radius fracture. In the past, surgery was required in 20% of cases. Currently, surgical indications are becoming more numerous due to titanium implants, given that these fixation materials allow for a snug fit, a quick recovery and have excellent functional results [2].

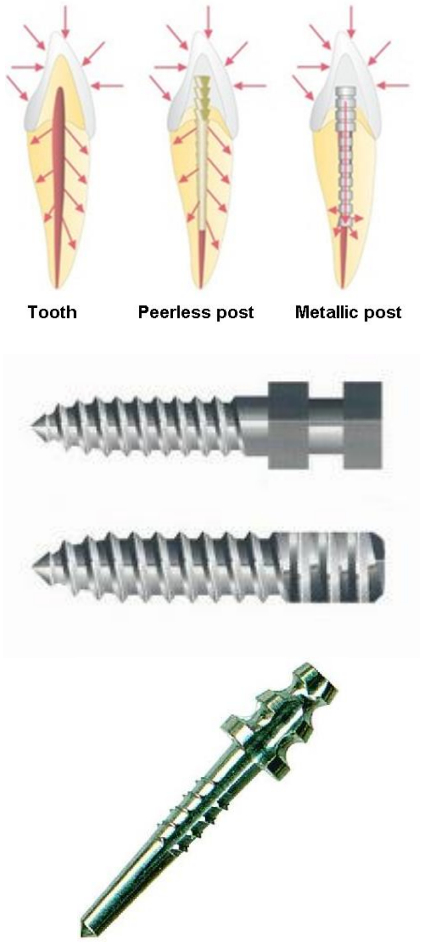


*Fig. 11. Titanium made post [20].*

The last example given in Fig. 11 shows some design of titanium posts. This example is very important because these implants made of the optimum variant of titanium powder resulting from the experiment presented above were used for an analysis of the induced stress in tissues by the metallic post [20].

### 4.4 A comparison of different post materials using finite element analysis

A 3D model of a tooth was created using ALGOR software. After selecting the type of finite element, the mesh was obtained manually [12], because it offers the possibility of controlling the numbers of finite elements in the areas with a high risk of fracture: cervical zone of the tooth and cervical third of the root. After the 3D model of an intact tooth was made, the root was separated in order to construct the 3D model of the tooth with a post-and-core system (Fig. 12). Fig. 13 presents the whole dental-periodontal complex.

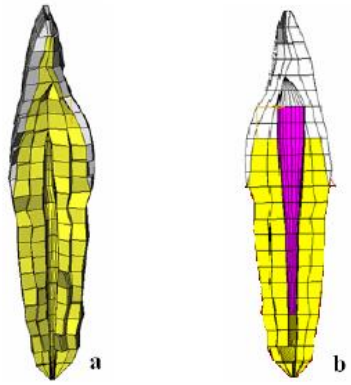


*Fig. 12. a) The 3D model of an intact tooth, b) The 3D model of a tooth with post-and-core system.*

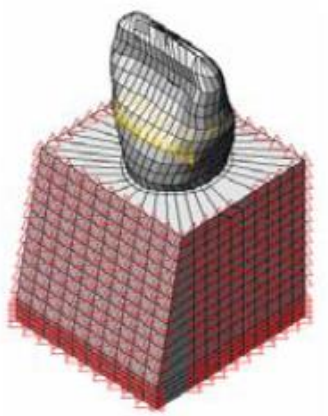

*Fig. 13. The final 3D model.*

The simulated load (30daN) was applied on the palatal surface of the crown, under an angle of 45 degrees to the long axis of the tooth (Fig. 14), evenly distributed to the loading area. The deformation limits are determined to ensure the equilibrium of the structure. The conditions differ between the two 3D models (intact tooth and reconstructed tooth with different post: ceramic, titan, carbon fiber post and glass fiber post) [13].

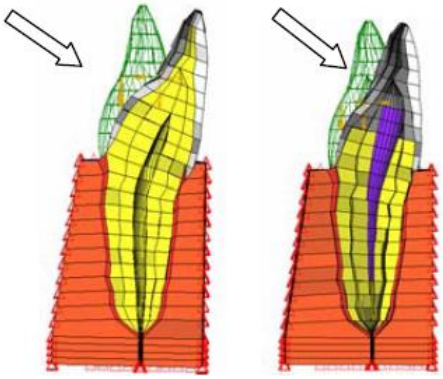

*Fig. 14. The load and imposed constrains.*

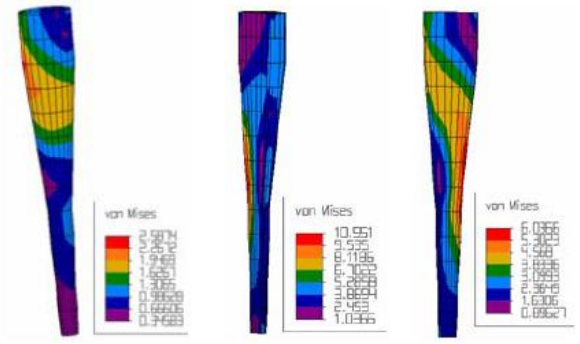


*Fig. 15. The von Mises stresses inside the models post: fiber post, ceramic post, titan post.*

Because of their material characteristics, carbon and glass fiber posts do not exhibit a great resistance to the applied load, but they have an enough elastic deformation before the rupture occurs. They determine the concentration of stress in the cervical third of the root, and this is an advantage for the longevity of the reconstruction. The rigid posts (ceramic and titanium) exhibit a superior strength in reference to the applied load, but the stress concentration area identified in the analysis is in the middle third of the root, at the post/dentine interface (Fig. 15).

## 5. Conclusions

- The current study includes theoretical process simulation of power production and identification of the process parameters. Based on this development, computer modelling of the whole process will be carried out to identify the main optimisation criteria.
- The experimental model is based on a multi-factorial experiment namely **complete central composite rotatable second order design $2^4$.**
- The data analysis shows that the best results occur at low feed and great current intensity. These influences are more pronounced for particles with 45 - 75 μm size range. In case of lower intensity values, the feed has virtually no influence on the process.
- The following optimum values for the technological parameters can be recommended: I – 250 A; U – 108 V; f – 400…450 mm/min; Q – 90…100 l/min.
- The optimum variant of the titanium powder was used for an analysis of the stress concentration for a dental post and comparison with using different types of materials for biomedical implants.

## References

[1] L. V. M. Antony, R. G. Reddy, Journal of Materials, March 2003.
[2] A. I. Bogdan, http://www.lectiadeortopedie.ro/implanturi-ortopedice/implanturi-pentru-humerus/, July 2014.
[3] I. Constantinescu, D. Golumbovici, D. Militaru, Ed. Tehnică, Bucureşti, 1980.
[4] S. Grenier, November 1998, Elsevier Science Ltd, 1997.
[5] S. Grenier, P. Tsantrizos, F. Allaire, Material Powder Report, November 1997, Elsevier Science Ltd, 1997.
[6] C. Key, http://www.mpif.org/apmi/doc4.htm, December 2012.
[7] J. Lezanski, Elsevier Science Ltd, 1997.
[8] Miomir G. Pavlovic, http://electrochem.cwru.edu/ed/encycl/art-p04-metalpowder.htm, December 2012.
[9] I. Nicolescu, http://www.gandul.info/magazin/premiera-medicala-o-mandibula-din-titan-realizata-cu-ajutorul-unei-imprimante-3d-a-fost-transplantata-cu-succes-unei-paciente-9213887, July 2014.
[10] C. Penescu, G. Ionescu, Ed. Tehnică, Bucureşti, 1971.
[11] Randal Bouverat, Advanced Materials & Processes, August 1999.
[12] M. F. Santini, V. Wandscher, M. Amaral, P. Baldissara, L. F. Valandro, Minerva Stomatol., **60**(10), 485 (2011).
[13] A. M. Viţalariu, R. Comăneci, , C. Dumitraş, J. Optoelectron. Adv. Mater. **9**(11), 3419 (2007).
[14] Yong-Hua Li, Zhen-Qian Sun, Xiao-Long Li, Pan-Pan Ding, Ling-Kai Gong, J. Optoelectron. Adv. Mater. **5-6**(16), 513 (2014).
[15] ***, Plasma atomisation process, accessible at http://www.pyrogenesis.com/powderatomization.htm December 2012.
[16] ***, Physical properties of titanium and its alloys http://www.key-to-metals.com/Article122.htm , February 2006.
[17] ***, Inorganic Powder / Particle Manufacture, http://www.reade.com/Particle_Briefings/powder_mfr.html, accessed at December 2013;
[18] ***, Patent 6565010, Hot gas atomization, http://64.233.183.104/search?q=cache:QEeXi4uFwkIJ:www.patentstorm.us/patents/6565010.html+%22Plasma+Atomization+gives+unique+spherical+powders%22&hl=ro, December 2012
[19] ***, http://www.biotechnic.ro/implanturi-spinale-solas/, July 2014
[20] ***, http://www.infodentis.com/pivot-dentar/caracteristici.html, accesed July 2014

*Corresponding author: razvancernat@gmail.com
dumitrascata@uahoo.com